

Magnetic properties of free-standing finite linear Co chains

J.C. Hernández-Herrejón and R. Chávez-Alcázar
Ingeniería en Nanotecnología UCEMICH,
Av. Universidad 3000 Sahuayo Michoacán 59103 México.
e-mail: jchernandez@ucienegam.edu.mx

Received 7 April 2018; accepted 3 May 2018

The ground state magnetic properties of Co_n linear atomic chains with $1 \leq n \leq 10$ are studied within density functional theory using the generalized gradient approximation. A linear scaling between the binding energy per atom and the inverse of the number of atoms in the chain is found. For the optimized geometries, our results show a dimerization effect for chains of few atoms but for the longer ones the phenomena disappear in the center but remains at the ends due to finite size effects. The spin moment, the orbital moment, and the magnetic anisotropy energy were investigated. For long chains, the orbital and spin moments have a tendency to become uniform. Enhanced spin and orbital moments were found due to the reduced coordination number compared to the cobalt in bulk. The cobalt chain of five atoms has the highest magnetic anisotropy energy with an outstanding 8 meV, suggesting that it could have applications in ultrahigh density magnetic memories and hard disk.

Keywords: Cobalt; linear chains; magnetism; moment.

PACS: 75.75.+a; 36.40.Cg; 75.30.Gw; 75.10.Lp

1. Introduction

Nanotechnology is a promising field because of the novel properties that the materials could display at nanoscale, more specifically magnetism at nanometer scale attracts considerable attention due to fundamental and technological perspectives [1-5]. For example, for high density magnetic recording one would likely be able to develop magnetic nanoparticles that combine both high saturation magnetization and large Magnetic Anisotropy Energy (MAE). The MAE determines the stability of the magnetization direction and the orientation of the magnetization with respect to the lattice structure. Also, magnetic nanoparticles offer great possibilities in biomedicine [6], for instance magnetic separation of labelled biological entities from its native environment using biocompatible nanoparticles, localized drug delivery reducing the side effects and the dosage, the possibility of treating cancer by induced hyperthermia dispersing magnetic nanoparticles throughout the target tissue and applying an external magnetic field, contrast enhancement agents for MRI and many more applications.

Theoretical research has been done in both infinite and finite linear chains of cobalt atoms. For freestanding infinite chains Guo and Tung [7,8] made a systematic *ab initio* study of the magnetic and electronic properties of all $3d$, $4d$ and $5d$ transition metals for both linear and zigzag nanowires, Kim *et al.* [9] with the WIEN97 code investigated the change in the electronic structure and magnetic moment of transition metals of group 8-10 as their dimensionality is reduced, they predicted that all are magnetic in 1D, except Ir. For finite linear chains Weinberger *et al.* [10] studied the magnetic properties of cobalt chains on Pt(111) and Bruno *et al.* [11] studied the structure and magnetic properties of cobalt chains on a stepped Cu surface. For cobalt monoatomic chains on top of the Cu(001) and Pt(001) see [12].

Nanostructures are not only a theoretical subject, experimental research has been done in the past years, linear Au_n chains with $1 \leq n \leq 20$ on NiAl(110) were created with the ability of a scanning tunneling microscope to manipulate single atoms [15]. Eigler and Schweizer [13] used a Scanning Transmission Microscope at low temperature to position individual Xe atoms on a single crystal nickel surface. Kern *et al.* [14] made various morphologies using diffusion-controlled aggregation on surfaces.

Heisenberg model calculations with finite range exchange interaction show that in a one dimensional chain, ferromagnetism cannot be maintained at finite temperature [16]. On the other hand, the inclusion of a strong magnetic anisotropy can modify this statement as was shown experimentally by Gambardella *et al.* [17], growing cobalt chains on a Pt(997) surface they showed evidence that in 1-D $3d$ metal chains can sustain both short and long range ferromagnetic order at a finite temperature. Cobalt has a strong tendency to magnetize due to their partially filled d -orbitals and exhibits magnetism in their bulk structures. For finite linear cobalt chains it is important to investigate the possibility of ferromagnetism at ground state. A lot of work has been done theoretically and experimentally but the understanding on the magnetic properties of freestanding finite linear cobalt chains and how magnetism affects their structural properties is still incomplete. At the best of our knowledge there is no such study.

In the present paper we study the magnetic properties of freestanding Co_n linear chains in the ground state with different length ($1 \leq n \leq 10$) in terms of *ab initio* calculations including the spin-orbit coupling (SOC). We focus on the spin moment, orbital moment and magnetic anisotropy. In Sec. 2 we describe our system and the computational method with the parameters used. In Secs. 3 and 4 we present our results of the binding energy, spin and orbital moments for the op-

timized chains and the magnetic anisotropy energy. Finally, we present our conclusions in Sec. 5. We study only free-standing chains but the physics of our results could also hold for other systems changing the values of the physical quantities, for example in break junctions, nanowires evolve to form a linear monoatomic chains when pulled along specific crystallographic directions [18-20].

2. Theory and computational Method

The calculations are performed in the framework of Hohenberg-Kohn-Sham's density functional theory [21] as implemented in the Vienna *ab initio* simulation package (VASP) [22]. This computer software solves the spin-polarized Kohn-Sham (KS) equations with an augmented plane-wave basis set that use the projector augmented wave (PAW) method [21,24], which is an approximate all-electron approach with frozen cores. The exchange and correlation effects are treated in the generalized-gradient approximation (GGA) by using the Perdew-Burke-Ernzerhof (PBE) functionals [23]. For *3d* transition metals, the electronic and magnetic properties are reliably described by considering as valence electrons the *3d*, *4s*, and *4p* states [24].

The cobalt chains are placed inside a supercell which dimensions are such that the interactions between neighboring images are negligible. In practice, this criterion is satisfied when the images are separated from each other by at least 12 Å. The KS wave functions in the interstitial region are expanded in a plane wave basis set with a kinetic energy cut-off of 575 eV, this value guarantees that the total energy converges within less than 1 meV/per atom. For metallic-like systems, one often finds very rapid variations of states close to the Fermi level that may cause a poor convergence of relevant physical quantities such as the total energy, therefore, a smearing of the KS levels is introduced in order to improve numerical stability. We have used a Gaussian smearing method with a standard deviation σ between 0.001 eV and 0.0002 eV, the σ value is different for each chain to keep the entropy of the non-interacting KS gas below 10^{-6} eV/K-atom. For small chains, $\sigma = 0.001$ is good enough to keep

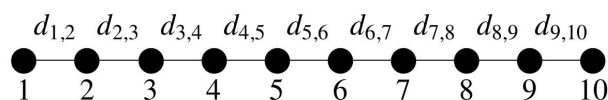


FIGURE 1. A representation of a Co_{10} chain. Also it could represent a smaller chain if we remove the last atoms, for instance this figure would represent a Co_8 chain if we remove the ninth and tenth atom. $d_{l,l+1}$ is the distance between l -atom and $(l+1)$ -atom.

the entropy low but it is not good for larger chains, in this case a smaller value around $\sigma = 0.0002$ is needed. Since we are dealing with isolated chains, the calculation of all Co_n chain properties is carried out by considering only the Γ -point in reciprocal space. The geometry optimization is performed by using the conjugate-gradient and quasi-Newton methods until all the forces on each atom are less than 0.001 eV/Å.

Figure 1 represents a linear Co_n chain with $n = 10$, $d_{l,l+1}$ is the distance between l -atom and $(l+1)$ -atom. For a chain with n atoms we have to compute $n - 1$ distances. The optimization is carried out in two stages, first we make a collinear calculation to obtain the charge density and then we use this charge to compute the energy including the spin-orbit coupling. The calculations are performed along the chain (Z axis) and perpendicular to the chain (X axis). Then we compute the magnetic anisotropy energy defined as the difference energy between X and Z axis. For the infinite linear chain we calculate the equilibrium bond length by computing the total energy in function of the interatomic distance and then locating the minimum. Finally we compute the MAE for the optimized geometries.

3. *Ab initio* results

3.1. Bond lengths and Binding energy

With the optimized structure coordinates we compute the distances $d_{l,l+1}$ for all chains. The calculated bond lengths for each chain are displayed in Table I, the first row indicates the amount of atoms in the chain and the first column indicates the distance between the l and $l+1$ atom in that chain. For

TABLE I. This table shows the distance between the l -atom and the $(l+1)$ -atom for the Co_n chains with $2 \leq n \leq 10$. The distance between any nearest neighbors in an infinite linear chain is 2.15 Å.

$n =$	2	3	4	5	6	7	8	9	10
$d_{1,2}$	1.96	2.12	2.00	2.02	2.02	2.00	2.02	2.02	2.02
$d_{2,3}$		2.12	2.56	2.25	2.26	2.31	2.27	2.27	2.32
$d_{3,4}$			2.00	2.25	2.10	2.10	2.14	2.13	2.09
$d_{4,5}$				2.02	2.26	2.10	2.16	2.20	2.18
$d_{5,6}$					2.02	2.31	2.14	2.20	2.16
$d_{6,7}$						2.00	2.27	2.13	2.18
$d_{7,8}$							2.02	2.27	2.09
$d_{8,9}$								2.02	2.32
$d_{9,10}$									2.02

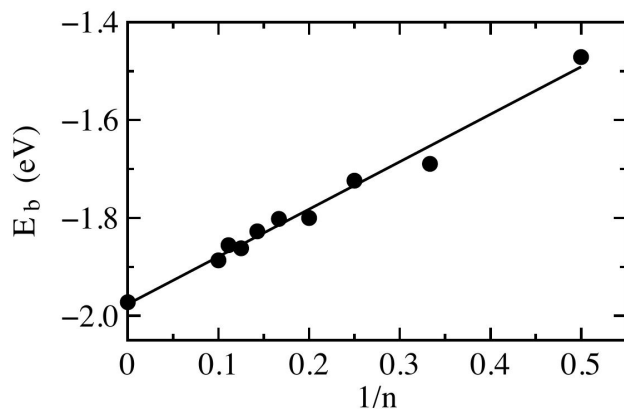


FIGURE 2. The binding energy per atom E_b in function of $1/n$. It follows a linear scaling in function of $1/n$ as $f(1/n) = -1.9759 + 0.9688(1/n)$.

instance, the trimer has $n = 3$, then $d_{1,2} = 2.12$ is the distance from atom 1 to atom 2 and $d_{2,3} = 2.12$ is the distance from atom 2 to atom 3. Also we computed the bond length for an infinite linear chain, the result is $d = 2.15$ Å.

We can see from Table I that for small chains a dimerization is generated, for long chains this effect almost disappears in the center but it is maintained at the ends of the chains. The dimerization effect is shown with more clarity for the chains of 4 and 10 atoms. For Co_4 the distance between atom 1 and 2 $d_{1,2} = 2.0$ Å and it is the same for $d_{3,4}$, but the distance between atom 2 and 3 is much bigger, $d_{2,3} = 2.56$ Å, then Co_4 apparently is made of 2 dimers. On the other hand, for Co_{10} the distances between the atoms near the center are almost the same, $d_{5,6} = 2.16$ Å, $d_{4,5} = d_{6,7} = 2.18$ Å and they are close to $d = 2.15$ Å that is the equilibrium bond length for a infinite chain. At the ends of the Co_{10} chain things are different, the distance between atom 1 and 2 $d_{1,2} = d_{9,10} = 2.02$ Å, but the distance between atom 2 and 3 is bigger $d_{2,3} = d_{8,9} = 2.32$ Å, thus the central atoms of the Co_{10} behaves like an infinite chain but there is a dimerization effect at the ends. The binding energy per atom E_b is defined as

$$E_b = (nE(1) - E(n))/n$$

where $E(1)$ is the energy of one cobalt atom and $E(n)$ is the Co_n chain energy, both energies are in ground state. Figure 2 shows E_b in function of the inverse number of atoms $1/n$ for the cobalt chains in the easy axis. Plotting E_b in function of $1/n$ allow us to represent the infinite cobalt chain binding energy at zero. We fit the data with the best straight line using the least squares method [25]. The line equation is $f(1/n) = -1.9759 + 0.9688(1/n)$, the value that is predicted for an infinite chain ($n \rightarrow \infty$) is -1.97 eV, it is the same value we calculated with VASP for the infinite chain binding energy. For small chains the fluctuations are not small with respect to the best straight line, this is because dimers and trimers are very different compared to an infinite chain and finite size effects are expected. While the chain is getting longer the fluctuations decrease, this shows a transition from the finite size chain to the infinite one. Only Co_2 and

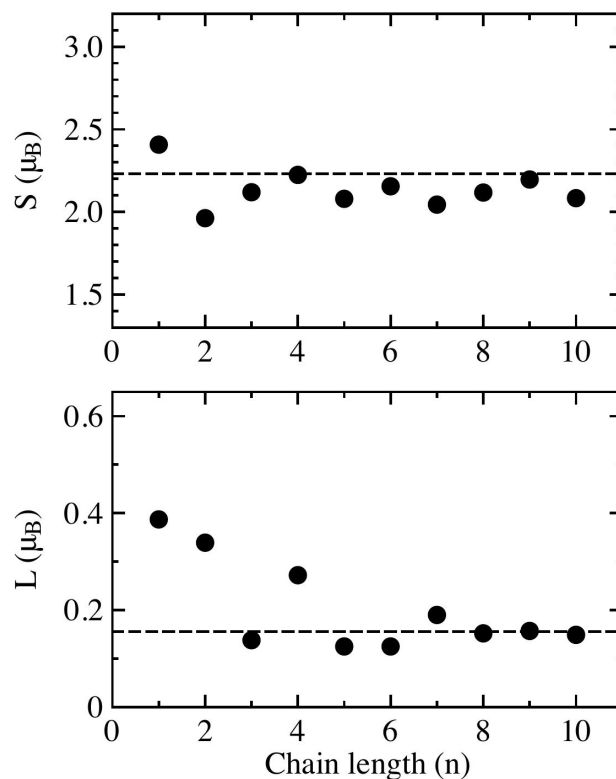


FIGURE 3. Calculated spin S and orbital moment L of the central (most symmetric) atom in Co_n ($n=1, \dots, 10$) chains for the easy axis. The dashed lines at 2.23 and 0.156 represent the S and L values for the infinite chain.

Co_4 chains have an easy axis in Z . All the Co_n chains with $n \geq 5$ have an easy axis in X in agreement with the infinite chain that also has the same easy axis.

3.2. Spin and orbital magnetic moments

The results of the spin moment S and orbital moment L in the easy axis for the central most symmetric atom in the cobalt chains are shown in Fig. 3. The upper graph shows the spin moment S in function of the length chain n , the dashed line at 2.23 is the spin moment S for an infinite linear chain. The single cobalt atom has the highest spin moment ($2.4 \mu_B$), it is around 10% higher than the corresponding infinite chain ($2.23 \mu_B$). On the other hand, the dimer Co_2 has the smallest S value ($1.96 \mu_B$). We notice that S fluctuates near the infinite chain spin moment and these fluctuations become smaller when the chain grows, for example the difference between the Co_9 central atom spin moment and the infinite chain is less than $0.02 \mu_B$. The behavior of the central atom spin moment S in Fig. 3 is similar to the behavior of S_z for Co_n chains deposited on Pt [10], in both cases fluctuations are high for small chains but decrease for the large ones, also the limiting value when $n \rightarrow \infty$ is similar, $S = 2.23 \mu_B$ for free standing chains and $S_z = 2.1 \mu_B$ for cobalt chains on Pt.

The lower graph of Fig. 3 shows the orbital moment L of the central atom in the cobalt chain in function of the length

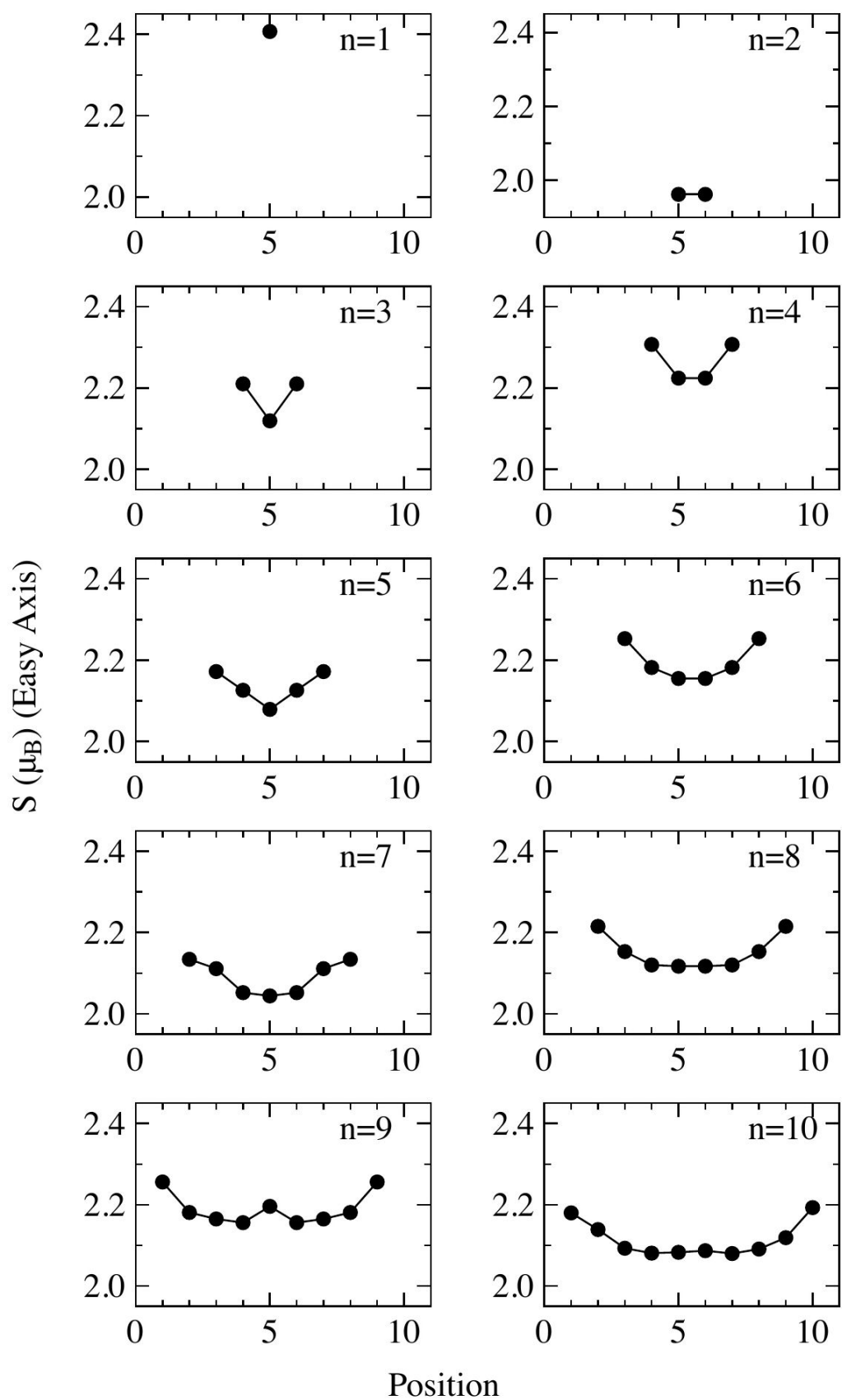


FIGURE 4. Spin moment of each atom in the chain in the easy axis.

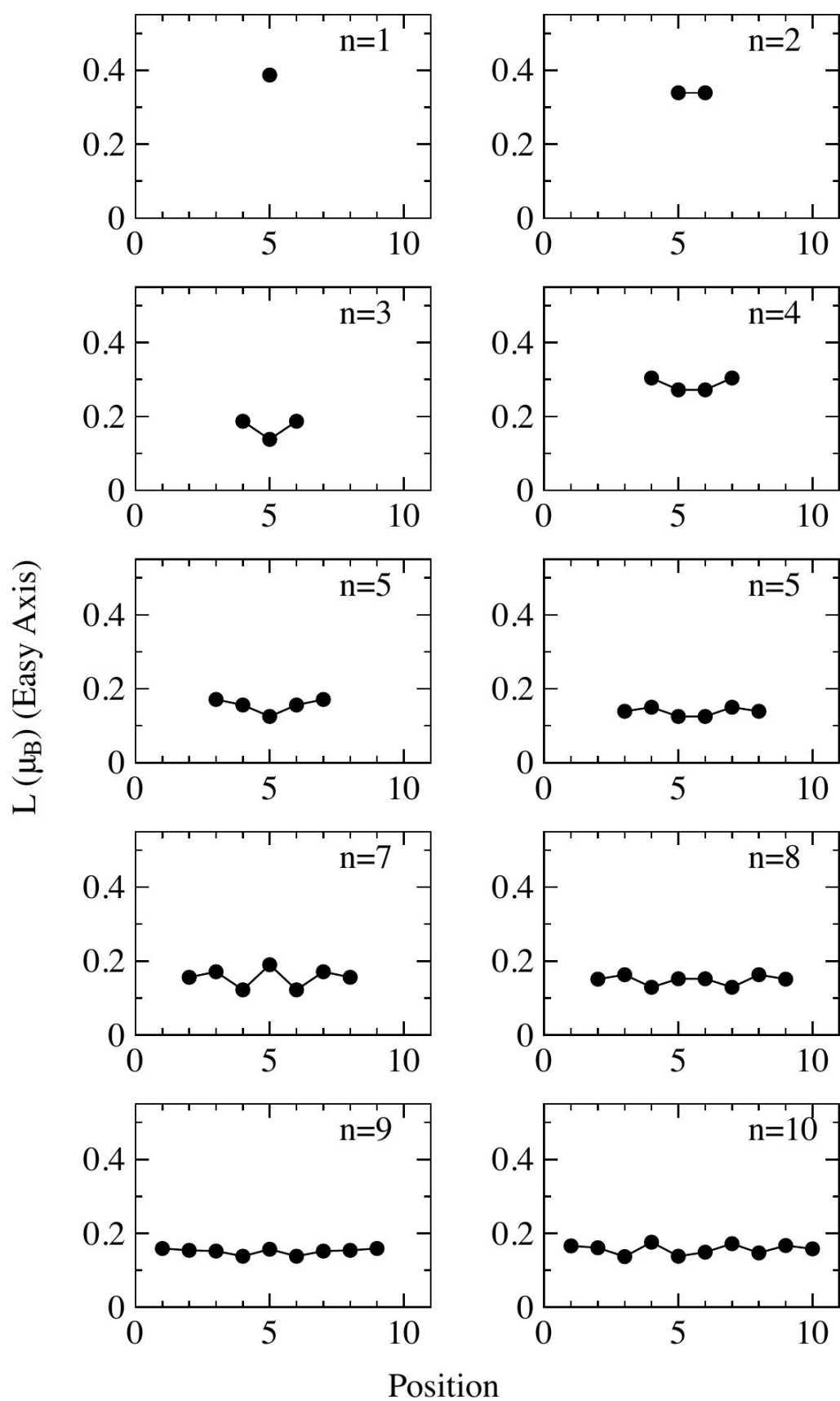


FIGURE 5. Magnetic orbital moment of each atom in the chain in the easy axis.

chain n , the dashed line at 0.156 is the orbital moment L for an infinite linear chain. First we notice that the single atom orbital moment $L = 0.39 \mu_B$ is more than the double of the infinite chain. The central atom orbital moment decreases with an increasing number of atoms forming the chain and stabilize very fast. The orbital moment fluctuates just a little in Co_n chains with $n > 4$, for example the orbital moment for Co_8 , Co_9 and Co_{10} are $L = 0.152 \mu_B$, $L = 0.157 \mu_B$ and $L = 0.149 \mu_B$ respectively. The three values are near to the infinite chain orbital moment $L = 0.156 \mu_B$. It is interesting to notice that the same behavior (not the values) is found for cobalt chains on Pt(111) [10], small chains have high L values but decrease as the chain is getting longer. For example the Co_n chains with $n = 8, 9, 10$ on Pt(111) have almost the same L value ($0.35 \mu_B$), it is a little bit more than the double of our result. The difference is because we are using freestanding chains meanwhile in [10] are using cobalt chains deposited on Pt.

The spin moment S of each atom forming the chain is shown in Fig. 4. We notice that the spin moments at the end of the chains for ($n=1,2,\dots,10$) are higher than those in the middle of the chains. Also the distribution of the spins becomes flat as the chain grows, except for Co_9 that has a small peak in the middle. The single cobalt atom has the highest spin moment $S = 2.4 \mu_B$ and the chain with the lowest values is Co_2 with a spin moment $S = 1.96 \mu_B$ per atom, the other chains belong to this interval. Figure 5 shows the orbital moment of each atom forming the chain. For Co_1 and Co_2 the orbital moment is near $L = 0.4 \mu_B$ and they are the chains with the highest values. For long chains the orbital moment has a tendency to become uniform. Comparing Fig. 4 and Fig. 5 we notice that the fluctuations of the orbital moment L are higher than the spin moment S fluctuations. A careful inspection of Fig. 3 shows that the central atom spin moment fluctuates around a value that is a little bit below the infinite chain spin moment, the reason is the central atom most of the times takes the smallest S value in the chain as we can see in Fig. 4.

4. Magnetic Anisotropy

We investigated the magnetic anisotropy energy, this is a very important characteristic in magnetic materials because it gives the magnetic moments orientation in the system and determines the stability of the magnetization direction with respect to external fields. We computed the magnetic anisotropy energy of cobalt chains between X axis and Z axis and we define the MAE as the energy difference between X and Z axis, thus positive and negative values are possible. Figure 6 shows the MAE per atom in function of $1/n$, in this case there is not a linear scaling, actually it is very irregular but apparently it decreases for long chains. For the Co_n chains with ($2 \leq n \leq 5$) the fluctuations of the MAE are high, but for cobalt chains longer than Co_4 , the MAE per atom tends to decrease (in absolute value) towards the MAE per atom of the infinite cobalt chain. Co_5 has increased the size

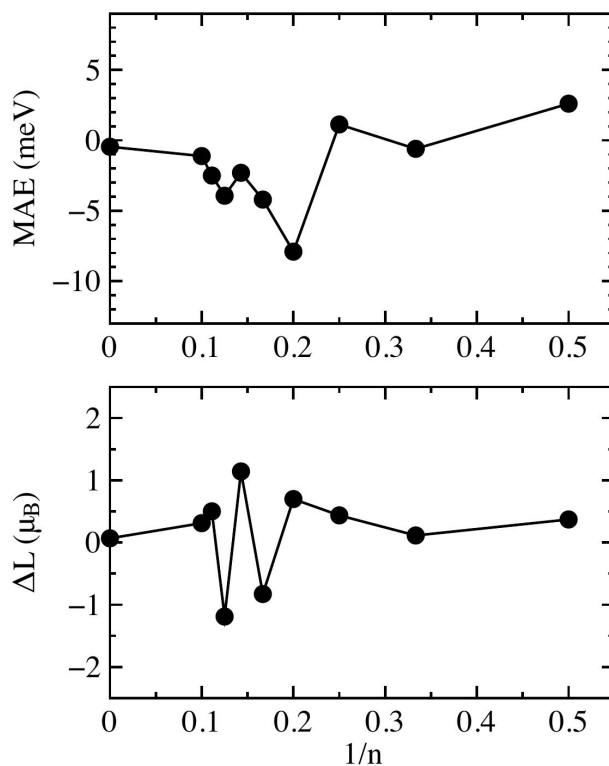


FIGURE 6. Upper graph shows the magnetic anisotropy energy per atom in function of $1/n$. Lower graph shows the difference of the orbital moment ΔL between the X and Z axis.

of the MAE with a value of -7.9 meV suggesting that it could have applications in ultrahigh density magnetic memories and hard disk. The lowest value is for Co_3 with -0.6 meV, it is a little bit higher (in absolute value) than the MAE for the infinite linear chain, 0.45 meV.

The lower graph in Fig. 6 shows the difference of the orbital moment ΔL between the X and Z axis. We investigated the validity of Bruno Model in cobalt chains. Bruno Model relates the difference of the orbital moment in the hard and easy axis with the MAE [26,27]. An inspection of Fig. 6 shows that there is no relationship between the MAE and ΔL , thus Bruno model cannot be applied in finite linear cobalt chains. In Co_9 and Co_{10} , both MAE and ΔL decreases, maybe for longer chains there is a relationship and Bruno model could be applied, we will investigate it later.

5. Conclusions

We studied the ground state magnetic properties of Co_n linear atomic chains with $1 \leq n \leq 10$, we found a linear scaling between the binding energy per atom and the inverse of the number of atoms in the chain. We found a dimerization effect in the chains, it is reduced in the center of big chains but holds at the ends. In the study of magnetic moments we showed the spin S and orbital L moments have a tendency to become uniform in large chains. An outstanding 8 meV magnetic anisotropy energy was found for Co_5 , it suggests applications

in ultrahigh density magnetic memories and hard disk. Investigating the MAE and ΔL we did not find evidence that Bruno Model works in finite linear Co_n chains with ($1 \leq n \leq 10$).

Acknowledgments

This work was supported by PROMEP F-PROMEP-39/Rev-04 and by computing time grants from CNS-IPICYT, TACC, LNS-BUAP.

-
1. S. Bedanta and W. Kleemann, *J. Phys. D: Appl. Phys.* **42** (2009) 013001.
 2. M.R. Fitzsimmons *et al.*, *Journal of Magnetism and Magnetic Materials* **271** (2004) 103.
 3. Hans-Benjamin Braun, *Advances in Physics* **61** (2012) 1.
 4. C. A. F. Vaz, J. A. C. Bland, G. Lauhoff, *Rep. Prog. Phys.* **71** (2008) 056501.
 5. F. J. Himpsel, J. E. Ortega, G. J. Mankey and R. F. Willis, *Advances in Physics* **47** (1998) 511.
 6. Q. A. Pankhurst, J. Connolly, S. K. Jones and J. Dobson, *J. Phys. D: Appl. Phys.* **36** (2003) R167.
 7. J. C. Tung, G. Y. Guo, *Phys. Rev. B* **76** (2007) 094413-1.
 8. J. C. Tung, G. Y. Guo, *Phys. Rev. B* **81** (2010) 094422-1.
 9. T. Nautiyal, T.H. Rho, and K.S. Kim, *Phys. Rev. B* **69** (2004) 193404-1.
 10. B. Lazarovits, L. Szunyogh, and P. Weinberger, *Phys. Rev. B* **67** (2003) 024415-1.
 11. S. Pick, P. A. Ignatiev, A. L. Klavsyuk, W. Hergert, V.S. Stepanyuk and P. Bruno, *J. Phys.: Condens. Matter* **19** (2007) 446001.
 12. J. Hong and R. Q. Wu, *Phys. Rev. B* **67** (2003) 020406-1.
 13. D. M. Eigler and E.K. Schweizer, *Nature (London)* **344** (1990) 524.
 14. H. Roeder, E. Hahn, H. Brune, J.P. Bucher and K. Kern, *Nature (London)* **366** (1993) 141.
 15. N. Nilius, T.M. Wallis, and W. Ho, *Science* **297** (2002) 1853.
 16. N. D. Mermin and H. Wagner, *Phys. Rev. Lett.* **17** (1966) 1133.
 17. P. Gambardella *et al.*, *Nature* **416** (2002) 301.
 18. E.P.M. Amorim, E.Z. da Silva, *Phys. Rev. B* **81** (2010) 115463.
 19. B. Ludoph and J.M. van Ruitenbeek, *Phys. Rev. B* **61** (2000) 2273.
 20. J. C. González *et al.*, *Phys. Rev. Lett.* **93** (2004) 126103-1.
 21. P. Hohenberg and W. Kohn, *Phys. Rev.* **136** (1964) B864; W. Kohn and L.J. Sham, *Phys. Rev.* **140** (1965) A1133.
 22. G. Kresse and J. Furthmüller, *Phys. Rev. B* **54** (1996) 11169; G. Kresse and D. Joubert, *Phys. Rev.* **59** (1999) 1758.
 23. J.P. Perdew *et al.*, *Phys. Rev. B* **46** (1992) 6671.
 24. P.E. Blöchl, *Phys. Rev. B* **50** (1994) 17953.
 25. R.L. Burden and J. Douglas Faires, *Numerical Analysis* 9-ed, (Brooks Cole, 20 Channel Center Street Boston, MA, USA, 2010), pp. 497-509.
 26. P. Bruno, *Phys. Rev. B* **39** (1989) 865.
 27. J. Stoehr and H.C. Siegmann, *Magnetism: From Fundamentals to Nanoscale Dynamics*, (Springer-Verlag, Berlin, Heidelberg, 2006), pp. 294-297.